Bull. Mater. Sci. (2021)44:68
https://doi.org/10.1007/s12034-021-02365-x

Efficiency enhancement in dye-sensitized solar cells with co-sensitized, triple layered photoanode by enhanced light scattering and spectral responses

G K R SENADEERA[1,2,*], D BALASUNDARAM[1,2], M A K L DISSANAYAKE[1], B A KARUNARATNE[3], A M J S WEERASINGHE[1], C A THOTAWATTHAGE[1], T JASEETHARAN[4], J M K W KUMARI[1] and D L N JAYATHILAKA[2]

[1]National Institute of Fundamental Studies, Kandy 20000, Sri Lanka
[2]Department of Physics, The Open University of Sri Lanka, Nawala, Nugegoda 10250, Sri Lanka
[3]Department of Material Technology, Faculty of Technology, Rajarata University of Sri Lanka, Mihintale 50300, Sri Lanka
[4]Department of Physical Sciences, Faculty of Applied Sciences, South Eastern University of Sri Lanka, Sammanthurai 32200, Sri Lanka
*Author for correspondence (gksen@ou.ac.lk)

MS received 24 August 2020; accepted 27 October 2020

Abstract. A method for impressive efficiency enhancement in TiO_2-based nanoparticle (NP) dye-sensitized solar cells (DSSCs) is demonstrated by using a co-sensitized triple layered photoanode, comprising a nanofibre (NF) layer of TiO_2 sandwiched between two TiO_2 P25 NP layers. Rose Bengal (RB) and Eosin-Y (EY) dyes are used for the co-sensitization. DSSCs with conventional TiO_2 (P25) NP bi-layer photoanode (NP/NP), sensitized with EY, showed an overall power conversion efficiency (η) of 0.89% under the illumination of 100 mW cm^{-2} (AM 1.5) with iodide-based liquid electrolyte. Whereas DSSCs fabricated with triple layered photoanode (NP/NF/NP) with the same total thickness and sensitized with EY yielded 1.77% efficiency under the same illumination conditions, showing an impressive $\sim$99% enhancement in the overall power conversion efficiency. The DSSCs fabricated with RB-sensitized NP/NP and NP/NF/NP photoanodes showed 0.25 and 0.73% efficiencies, respectively. Upon optimization, DSSCs fabricated with co-sensitized NP/NP bi-layer and NP/NF/NP triple layer photoanodes showed 1.04 and 2.09% efficiencies, respectively, showing again an impressive $\sim$100% enhancement in η due to the co-sensitized triple layer photoanode structure. Increase in the short circuit photocurrent density, UV–visible absorptions measurements, incident photon to current efficiency and electrochemical impedance spectroscopic measurements confirmed that this enhancement is very likely due to the enhanced light harvesting and reduction of recombination of photoelectrons combined with the enhanced spectral responses of the co-sensitized triple layered photoanode.

Keywords. Dye-sensitized solar cells; co-sensitization; light scattering; electrospun nanofibres; triple layered photoanode.

1. Introduction

Dye-sensitized solar cells (DSSCs) have attracted a considerable interest over the conventional photovoltaic devices during the recent past, due to their promising characteristics such as low manufacturing cost, flexibility, low weight and design opportunities [1–5]. Conventionally, photoanodes of DSSCs consist of 10–15 μm thick TiO_2 thin films having nanocrystals with diameters of 15–30 nm size providing a large specific surface area for optimal dye adsorbing [2], which is an essential factor for achieving higher efficiencies in DSSCs. Many efforts have been carried out in the recent past to enhance the efficiencies of these DSSCs by applying different techniques. Among the techniques available to enhance the efficiencies of these DSSCs is the light trapping in the photoanode by increasing the light scattering within the photoanode [6,7]. Therefore, in order to obtain both large surface area and enhanced light scattering in DSSCs, usually an additional light scattering layer consisting with larger particle in 200–400 nm range is used [8–11]. In this context, many people have tried bilayer structured photoanodes such as nanoparticles [7–12], nanorod aggregate [13,14], nanofibres (NFs) [15], nanotubes [16], nanospheres [17], etc. Recently our group has introduced three-layered structure of photoanode by using either electrospun NFs or nanorods obtained by electrophoresis [18–20], showing enhanced efficiencies in DSSCs due to improved light scattering in the photoanode. Apart from the

Published online: 23 March 2021

efficient light absorbing by the photoanode, spectral response of dye is another crucial factor determining the efficiency of DSSC. Partial absorption coverage by the dyes is still a major problem of achieving high efficiencies in DSSCs. Since it is difficult to synthesis a dye that can absorb the photons in the full solar spectrum, researchers have introduced co-sensitization method using more than one dye, broadening the wavelength range of absorptions in the solar spectrum while increasing the incident photon to current conversion efficiency (IPCE) of the DSSC [21–26]. However, even though large numbers of papers have been published on co-sensitization and inclusion of different types of light scattering layers in the photoanode fabrication, to the best of our knowledge there has been no study on the utilization of combined effect of above concepts towards the efficiency enhancement in the DSSCs, especially with the triple layer structure of photoanode. Therefore, in order to establish this new concept, in this study we have selected two different spectral complementary dyes together with a triple layered structure, in which the middle layer consists with electrospun NFs, providing a large surface area for increase in dye adsorption as well as the light scattering inside the photoanode. Impressive $\sim$100% efficiency enhancement is achieved by combining the above two concepts.

2. Experimental

2.1 *Preparation of composite triple layer TiO_2 photoanode*

Triple layered nanocrystalline TiO_2 electrodes were prepared by following the method described by us in the literature [18–20]. At first, a thick TiO_2 nanoparticle (NP) layer deposited on fluorine-doped tin oxide (FTO) conducting glass substrate (Solaronix, 8 Ω sq^{-1}, Switzerland; FTO) by 'doctor blade' method was arranged. The paste was prepared with 0.25 g of TiO_2 powder (Degussa P-25), 1 ml of 0.1 HNO_3 (Fluka), 0.05 g of PEG (Sigma Aldrich), 1 drop (0.2 ml) of Triton-X 100. A creamy homogeneous paste was obtained by grinding these materials for 45 min. A thin film of TiO_2 NP was then doctor bladed on FTO and sintered at 450°C for 45 min and cooled down to the room temperature. Then intermediate TiO_2 layer of NF was introduced according to the method described in the next section. After that in order to make the triple layered photoanode structure, another layer of TiO_2 (P25) was applied on top of the NF layer by the same method as mentioned previously. Finally, electrode with FTO/NP/NF/NP TiO_2 photoanode structure was obtained. For the comparison, electrodes with FTO/NP/NP were also prepared with the same thickness as in the triple layer structure. Finally, these two types of photoanodes were dipped separately in an ethanolic Eosin-Y (EY) dye and Rose Bengal (RB) dye solution of 0.3 mM for 24 h. In order to do the co-adsorption of dyes, TiO_2 electrodes were dipped in a mixture of (1:1) RB and EY dye solutions, respectively, for 12 h. The effective area of each photoanode was kept as 0.25 cm^2.

2.2 *Preparation of TiO_2 NF layer*

Solution for the electrospinning was prepared as follows. Polyvinyl acetate (PVA), 1.5 g, was mixed with 3 g titanium (iv) isopropoxide (TIP, Fluka) with 1.2 g of acetic acid (Sigma Aldrich) as a catalyst for sol–gel reaction. Then 19 ml of N,N-dimethylforamide (DMF, Sigma Aldrich) was added and solution was magnetically stirred for 4 h. A substrate of FTO glass with a sintered TiO_2 NP layer was then fixed to the Nabond electrospinner (China) and the distance between the syringe tip of the spinner and the drum with the substrate was kept as 6.5 cm. The solution was then electro spun on to the substrate with a spinning speed of 270 rpm. The flow rate was kept at 2 ml h^{-1} and electrospinning time was 20 min. The substrate with deposited TiO_2 NF membrane was then sintered at 450°C for 1 h.

2.3 *Morphological characterization of TiO_2 films*

The surface morphology and the sizes of the NPs and NFs were carried out using ZEISS EVO scanning electron microscope. Energy-dispersive X-ray (EDX) spectra were obtained from Ametek EDAX module with Octane T Optima-60 EDX detector.

2.4 *Preparation of the electrolyte*

A quantity of 0.738 g of tetrapropylammonium iodide (Pr_4NI) was dissolved in a mixture containing 1.0 ml of acetonitrile (Sigma Aldrich) and 3.6 ml of molten (MP 40°C) ethylene carbonate. Then 0.060 g of I_2 was added to the solution and it was stirred for 5 h.

2.5 *Cell assembly and I–V characterization*

In order to compare the performance of DSSCs with TiO_2 NP/NP bilayer and TiO_2 NP/NF/NP triple layer photoanode, DSSCs were fabricated with respective photoanode configurations having the same thickness and same effective area, as schematically shown in figure 1. Devices were fabricated by sandwiching the dye-adsorbed photoanodes with platinum-coated FTO counter electrode placing a few drops of the electrolyte in between the dye-adsorbed TiO_2 photoanodes and the platinum-coated FTO counter electrode. Photovoltaic characteristics of DSSCs were obtained by using a computer-controlled setup consisting of a solar simulator, coupled to a Keithly 2000 multimeter and a potentiostat/galvanostat HA-301 under the illumination

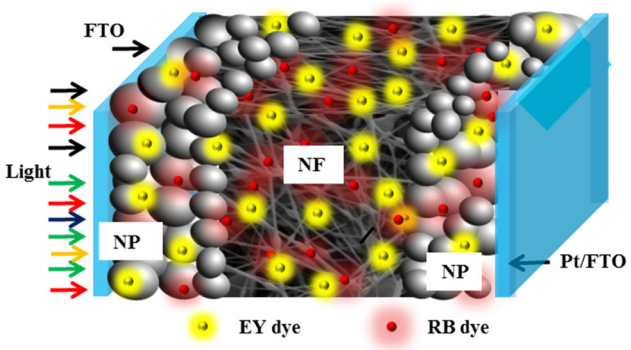

Figure 1. Schematic diagram showing structure of the co-sensitized DSSC with FTO/NP/NF/NP/Pt-FTO configuration.

of 100 mW cm^{-2} using a Xenon 500 lamp with an AM 1.5 filter.

2.6 *EIS measurements*

Electrochemical impedance spectroscopic (EIS) measurements were performed on DSSCs with both types of photoanodes under the same illumination of 100 mW cm^{-2}. Metrohm Autolab Potentiostat/Galvanostat PGSTAT 128 N with a FRA 32 M Frequency Response Analyzer (FRA) was used to obtain the impedances spectra of both devices in the frequency range between 1 MHz and 0.01 Hz.

3. Results and discussions

Surface morphologies of photoanode were examined by scanning electron microcopy (SEM). Figure 2a shows the top view of the NP TiO_2 layer. As depicted in the figure, porous structure of NP layer consists of TiO_2 NPs with an average diameter of 40 nm. Figure 2b and c depicts the SEM photographs of TiO_2 NF layer before and after sintering at 450°C, respectively. According to figure 2b, before sintering, TiO_2 NF layer appears to consist of a randomly distributed heavily interconnected 3D network. The average diameter of an individual fibre is around 200 nm. However, after sintering, the shape of the NF has changed to a rice grain-shaped elongated bead-type nanostructure with two sharp pointed ends. The average length and the diameter of these rice grains are ∼260 and 70 nm, respectively. In our previous reports, it was already reported that the NFs in the middle layer of the triple layer photoanode structure enhances the availability of light photons for the dye molecules to be excited, due to the multiple scattering effects within the NF layer as well as in the interface between the NP/NF layer [18–20]. Figure 2d shows the SEM image of the cross-section of the NP/NP layered photoanode fabricated with the same thickness as in the NP/NF/NP tri-layer structure. The overall thickness was controlled by using a mechanical setup in the doctor blade method. According to this figure, the estimated total thickness of the NP/NP layered photoanode structure appears to be around 21 μm. Since the optimized thickness of the NF layer used in the DSSC was very small, it was not practically possible to get a clear undamaged cross-section of the NP/NF/NP structure for SEM imaging. However, the experimental conditions we have used during the formation of NFs by electrospinning, such as flow rate, concentration and the viscosity of the precursor solution, drum speed with the substrate, the distance between the tip of the spraying nozzle and the substrate and the supplied voltage, the thickness and the formation of the NF would be uniform and approximately 1.5 μm thick, as observed in one of our previous studies [18,19].

Figure 3a and b shows the EDX spectra of TiO_2 P25 NPs and TiO_2 NFs after sintering at 450°C for 45 min. The EDX spectrum of TiO_2 NFs clearly shows the same features of TiO_2 NPs and it confirms the presence of the elements Ti and O without any impurity element. The peaks around 0.2, 0.3 and 4.3 keV are corresponding to the binding energies of titanium and oxygen related to the TiO_2 NPs as observed by Sundrarajan *et al* [27].

UV–visible absorption spectra of the above two types of TiO_2 layers sensitized with RB and EY are shown in figure 4. As can be seen from the figure, both TiO_2 layers with eosin dye (curves (a) and (c)) show a prominent peak around ∼525 nm. The films with RB shows (curves (b) and (d)) significant light absorption around 575 nm. Since the other physical parameters of the electrodes such as area, concentrations of the dye solutions, dipping time, etc., are kept constant, the absorption of these curves can be directly compared with their degree of light absorption. Therefore, as it can be clearly seen from the figure, light absorption by the two different dyes of the TiO_2 films prepared with NP/NF/NP structure is superior to that of the films prepared with NP/NP structure. Since all the absorption values were normalized with the mass of the photoanode for this comparison, the light absorbance enhances only in the peak areas without shifting the full curve. This enhanced light absorption in the NP/NF/NP structure could be attributed with the enhanced light scattering due to the incorporation of the NF layer in the TiO_2 electrode.

Performances of the DSSCs fabricated with the above two photoanodes having the same thickness but sensitized with EY and RB under the illumination of 100 mW cm^{-2} are shown in figure 5. Curves (a) and (b) show the current–voltage (*J–V*) characteristics of the devices with NP/NP photoanode structure sensitized with EY and RB, respectively, whereas curves (c) and (d) show the *J–V* characteristics of the DSSCs with NP/NF/NP triple layer photoanode structure sensitized with the same dyes, respectively. By comparing the photocurrent density values of curves (a) and (c), in the figure, a remarkable increase in photocurrent density can be seen for the DSSCs fabricated with NP/NF/NP structure and sensitized with the EY dye. A similar trend can be seen in the curves (b) and (d), which

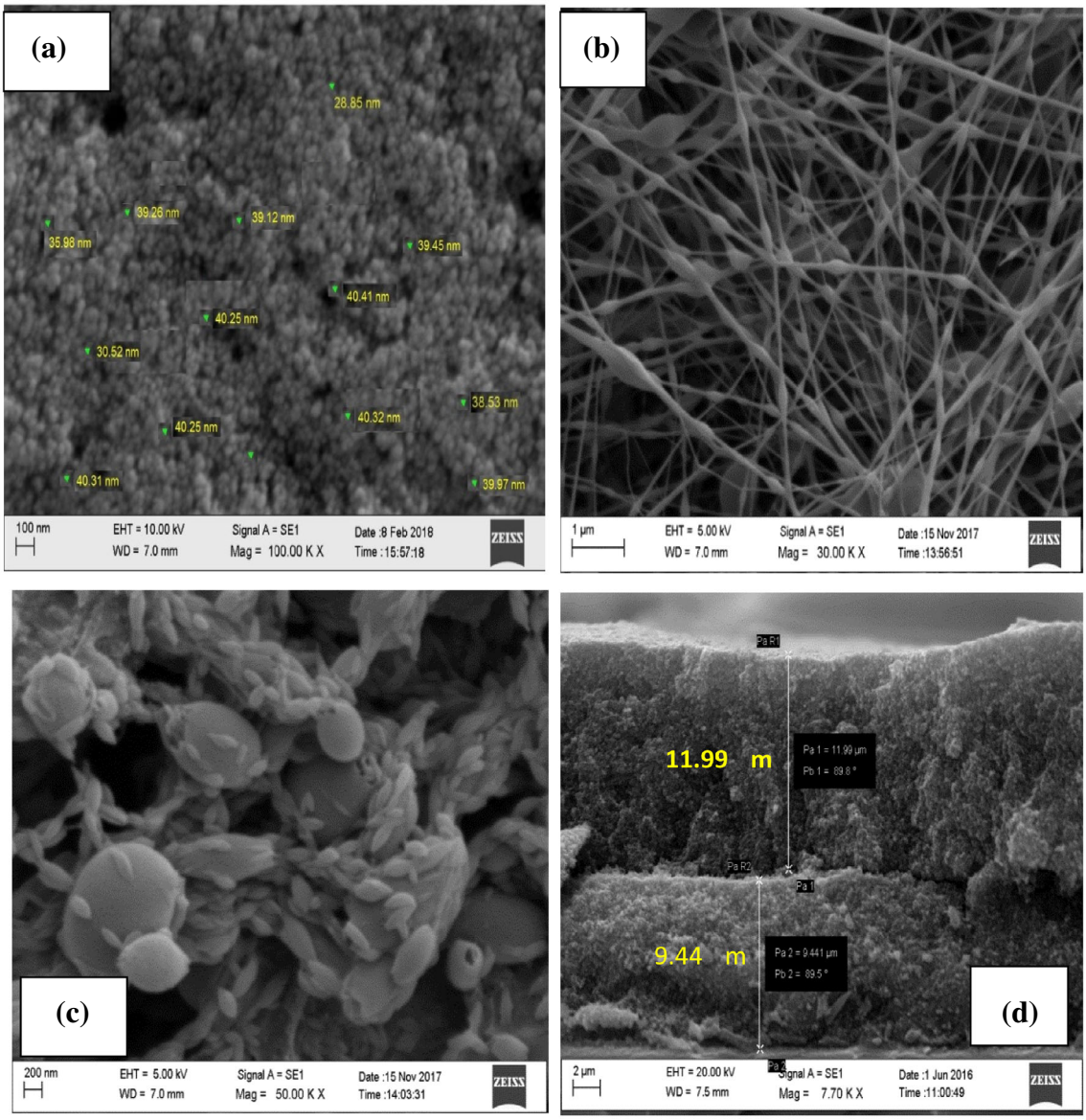

Figure 2. SEM images of TiO_2 photoanodes: (**a**) NP layer, (**b**) NF layer before sintering, (**c**) NF layer after sintering and (**d**) cross-sectional view of FTO/NP/NP photoanode.

were obtained from the DSSCs with photoanodes sensitized with RB dye too. Therefore, it is evident that, DSSC fabricated with triple layered structure shows superior solar cell performances compared to the DSSC fabricated with NP/NP photoanode structure. Device parameters namely, the short-circuit photocurrent density (J_{SC}), open-circuit voltage (V_{OC}), fill factor (FF) and the energy conversion efficiency (η) estimated from the above J–V curves of the above DSSCs fabricated with and without the NF layer are tabulated in table 1.

As it is evident from table 1, the photovoltaic performances have improved due to the incorporation of the NF interfacial layer. The highest efficiency of 1.77% is achieved from the DSSC with EY-sensitized NP/NF/NP photoanode, which is nearly 100% higher than that of the device assembled with only NP layers (NP/NP) with the same thickness. The J_{SC} and V_{OC} values also exhibit the same trend and the highest J_{SC} and V_{OC} are 3.98 mA cm^{-2} and 662 mV with the NF-based DSSC. Similar trend even with higher percentages can be observed with the DSSCs sensitized with RB dye. This improvement in photovoltaic performance of NP/NF/NP-based DSSC could be attributed to the enhanced light absorption by increased light scattering within the triple layer photoanode structure as well as due to the improved dye loading on the surface of the tri-layer TiO_2, photoanode structure.

Figure 6 shows the normalized UV–visible absorption spectra of the individual dyes together with the mixture in

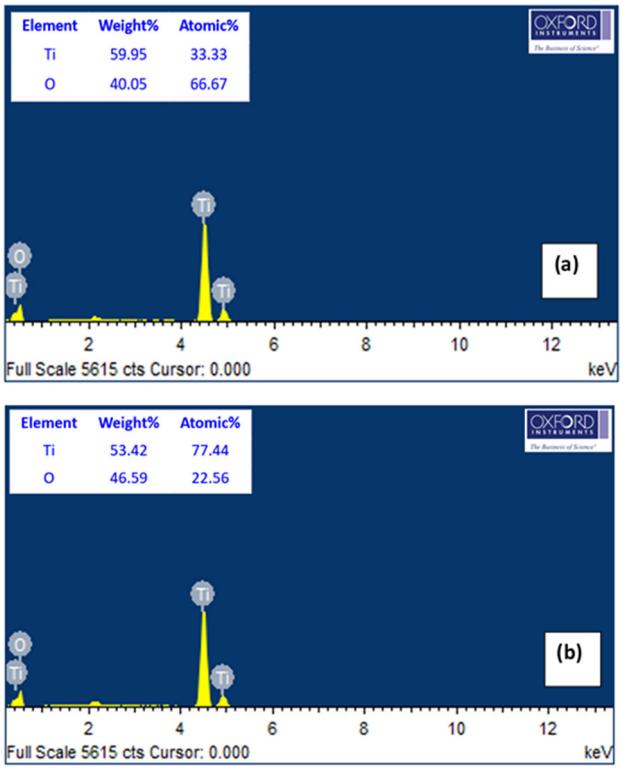

Figure 3. Energy dispersive X-ray spectra of (**a**) TiO_2 P25 nanoparticles and (**b**) TiO_2 nanofibres after sintering at 450°C for 45 min.

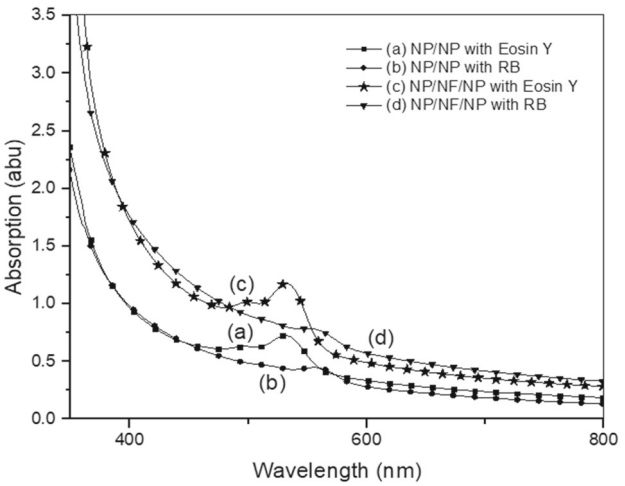

Figure 4. UV–visible absorption curves for (**a**) NP/NP with EY, (**b**) NP/NP with RB, (**c**) NP/NF/NP with EY and (**d**) NP/NF/NP with RB.

ethanol. According to the curve (i) RB dye in ethanol shows two peaks, one at ∼518 nm and the other at ∼559 nm. Similarly, EY (ii) shows two absorption peaks at ∼475 and ∼525 nm in ethanol. As it is evident from the curve (iii) in the figure, mixture of two dyes in equal amounts and concentrations shows corresponding peaks related to the individual dyes confirming the increase in the light absorptions

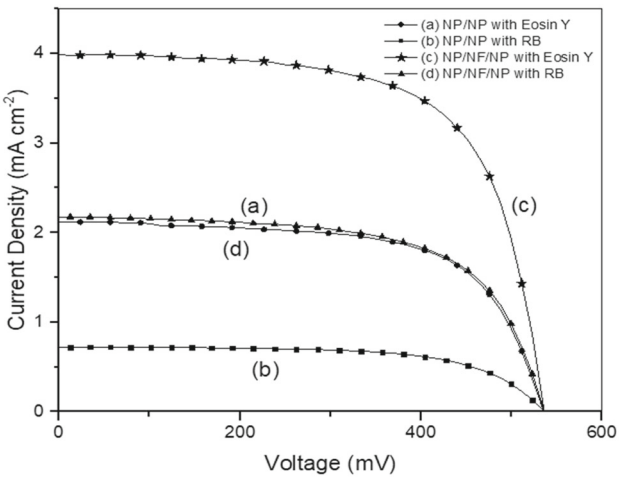

Figure 5. Current–voltage curves of DSSCs either with EY or RB sensitized photoanodes: (**a**) NP/NP/EY, (**b**) NP/NP/RB, (**c**) NP/NF/NP/EY and (**d**) NP/NF/NP/RB.

with broadening of the spectral responses. In order to see the actual light absorption phenomenon of the co-sensitized photoanodes with different structures, UV–visible absorption spectra of co-sensitized photoanode structures of NP/NP and NP/NF/NP were also obtained and depicted in figure 6. As it can be seen from curves (a) and (b), absorption spectra of both photoanodes show peaks corresponding to the individual dyes shouldering at ∼525 nm and 562 nm with small red shift due to the attachment with the TiO_2 surface. However, overall absorption of the triple layered photoanode was little higher than that of the photoanode without the NF layer.

Figure 7 shows current–voltage characteristics of the DSSCs with co-sensitized photoanodes, comprising with either NP/NP or NP/NF/NP under the same light irradiation with intensity of 100 mW cm^{-2}. As it is evident from the figure, the performances of DSSCs with NP/NF/NP photoanode is much higher than that of the DSSCs with NP/NP photoanode.

Photovoltaic parameters estimated from the curves in figure 7 are tabulated in table 3. The co-sensitized DSSC with NP/NP photoanode shows a power conversion efficiency (η) of 1.04% with V_{OC} of ∼613 mV, J_{SC} of 3.02 mA cm^{-2}, and FF of 61%. Whereas the DSSC fabricated with triple layered photoanode shows a power conversion efficiency (η) of 2.09%, with J_{SC} of 4.66 mA cm^{-2}, V_{OC} of ∼641 mV and FF of 64% with an average efficiency enhancement by two-fold and ∼54% enhancement in current density. The improved performances of DSSC with NP/NF/NP can mainly be attributed to the higher value of J_{SC} due to the enhanced light absorption by scatterings due to the insertion of the NF layer in the photoanode structure as well as due to increased dye loading. Meanwhile, a higher FF of the DSSC with triple layer implies that the surface recombination was reduced at the electrode/electrolyte interface through a better coverage of TiO_2 surface by both

Table 1. Photovoltaic parameters of DSSCs with different photoanode structures.

Dye	Type of photoanode	J_{SC} (mA cm^{-2})	V_{OC} (mV)	FF	η%
Eosin-Y	NP/NP	2.14 ± 0.10	645.5 ± 2	64 ± 1	0.89 ± 0.01
	NP/NF/NP	3.98 ± 0.25	662.2 ± 1	64 ± 2	1.77 ± 0.02
Rose Bengal	NP/NP	0.72 ± 0.10	537.1 ± 3	64 ± 2	0.25 ± 0.01
	NP/NF/NP	2.12 ± 0.30	550.5 ± 2	65 ± 2	0.73 ± 0.02

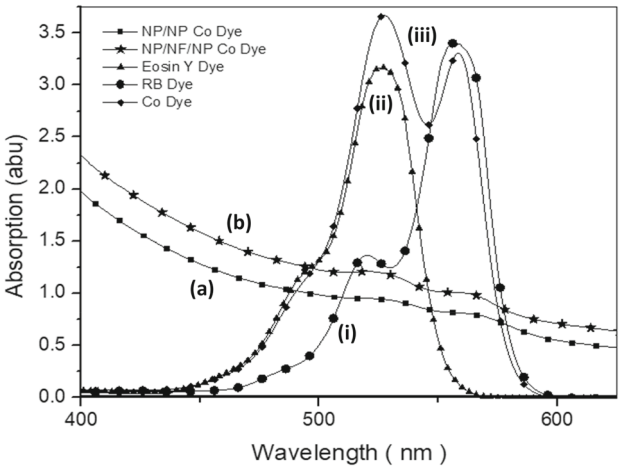

Figure 6. UV–visible absorption spectra of EY and RB in (**a**) ethanolic solutions and (**b**) in photoanodes (i) RB, (ii) EY and (iii) co-dye solution (RB+EY).

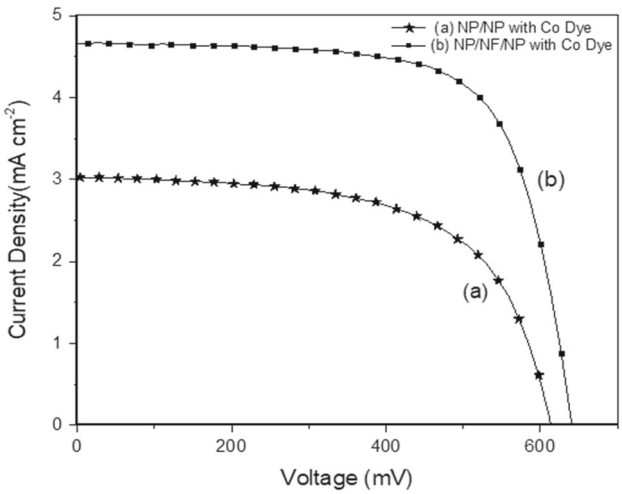

Figure 7. Photocurrent–voltage curves for DSSCs fabricated with (**a**) TiO_2 NP/NP control photoanode and (**b**) TiO_2 NP/NF/NP triple layer photoanode.

dyes with different sizes. The V_{OC} is also enhanced because of the increase in the Fermi level in TiO_2 with the increase of the amount of electrons injected from the double dye into the conduction band of the TiO_2 [28–30]. Mathematically this can be proved by using the formula mentioned by Zaban *et al* [31] with the quasi Fermi level of the electrons in the semiconductor photoanode under illumination (E_{Fn}), the potential of the Redox electrolyte (E_{Redox}), together with the positively elementary charge (e) as follows:

$$V_{OC} = \frac{E_{Fn} - E_{Redox}}{e} = \frac{k_B T}{e} \ln\left[\frac{n}{n_0}\right]$$

It can be further elaborated by using the terms thermal energy ($k_B T$) and the electron concentration in the conduction band of the semiconductor photoanode under illuminated conditions, n and the electron concentration under dark conditions n_0 as depicted in above formula. Therefore, as it was observed from the enhanced J_{SC}, due to the increase in charge transfer efficiency more electron accumulations in the conduction band of TiO_2 was detected. This could result in an increase of n, while the E_{Redox} value remains unchanged due to the same electrolyte used in all the above solar cells. Therefore, clearly V_{OC} is expected to be improved in the DSSCs with NP/NF/NP photoanode [31,32] (table 2).

Since the DSSCs with triple layer electrode shows higher photovoltaic performances than with the conventional type NP/NP electrode, in order to see the effect of co-sensitization on the spectral responses of the photoanode, IPCE spectra as a function of the wavelength of the DSSC with co-sensitized with NP/NF/NP photoanode were obtained. Figure 8 shows corresponding IPCE spectra of photoanode with NP/NF/NP structure sensitized with RB, EY and (RB+EY) dyes. As depicted in curve (a), RB dye shows IPCE peaks at ∼525 and ∼565 nm with broad spectral response covering the wavelength range between 450 to 600 nm, correlated with the UV–visible absorption spectrum of the RB dye as shown in figure 7. On the other hand, EY dye produces a broad IPCE spectrum within 450 to 575 nm region with two peaks at ∼475 and 550 nm again correlating with the UV–visible absorption spectrum of it (figure 7). It is interesting to note that, both IPCE and UV–visible absorption values corresponding to EY dye is much higher than that of the RB dye. Since the IPCE corresponds to the number of electrons measured as photocurrent in the external circuit, divided by the monochromatic photon flux that strikes on the cell, this enhancement in IPCE is very well interrelated with the higher short-circuit current density and output voltage of the EY dye-sensitized photoanodes, when it is compared with the RB-sensitized photoanodes, as depicted in figure 7. The co-sensitized

Table 2. Photovoltaic parameters of co-sensitized DSSCs with different photoanodes.

Type of co-sensitized photoanode	J_{SC} (mA cm^{-2})	V_{OC} (mV)	FF	η%
NP/NP	3.02 ± 0.2	612.6 ± 2	61 ± 1	1.04 ± 0.05
NP/NF/NP	4.66 ± 0.3	640.9 ± 3	70 ± 1	2.09 ± 0.04

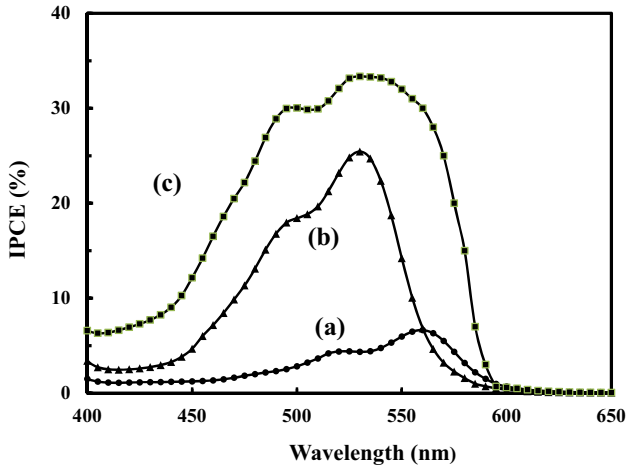

Figure 8. The IPCE spectra of DSSCs with NP/NF/NP photoanode sensitized with (**a**) RB, (**b**) EY and (**c**) RB + EY dyes.

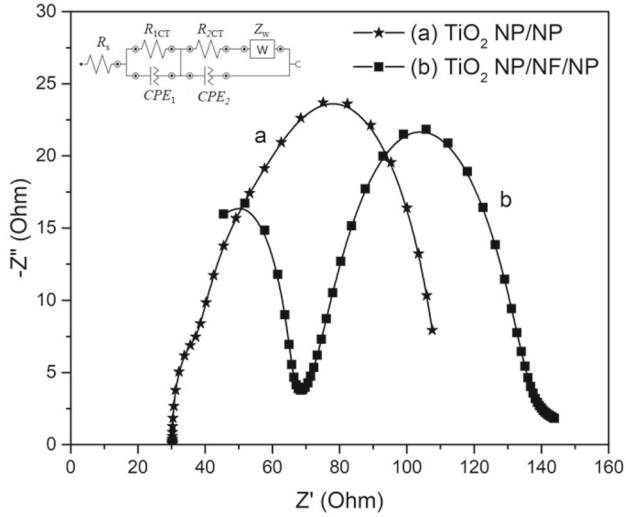

Figure 9. Impedance spectra of (**a**) TiO_2 NP/NP and (**b**) TiO_2 NP/NF/NP photoanodes and the equivalent circuit used to estimate the interfacial resistance of the devices.

RB + EY based DSSC showed a broad IPCE spectrum from ~425 to ~600 nm showing that peak positions correspond to the individual dyes. The IPCE of the co-sensitized photoanode is ~34% at around 525 nm and approximately 1.5 times higher than that of the EY dye. The observed IPCE enhancement in the co-sensitized photoanode may be attributed to the improved charge collection efficiency due to the different spectral responses of individual dyes as well as the efficient light trapping in the NP/NF/NP structure, as revealed by J_{SC} values of DSSCs fabricated with two different types of photoanodes (figure 8).

Electrochemical impedance spectroscopy (EIS) has been regarded as a powerful technique to characterize the carrier transport, electronic and ionic processes and recombination in DSSCs. Figure 9 shows the Nyquist plots of the co-sensitized DSSCs with FTO/NP/NF/NP/Pt-FTO and FTO/NP/NP/Pt-FTO configurations together with the equivalent circuit (inset) used to estimate the corresponding interfacial resistances of the devices. As it is depicted in the figure, two characteristic semicircles including a smaller one at higher frequency and a larger one at intermediate frequency can be seen. As it is well known, the smaller semicircle is fitted to the charge transfer resistance R_{1CT} should be ascribed to the process at the electrolyte/Pt counter electrode interface. The larger semicircle in the intermediate frequency region is associated to the charge transfer resistance (R_{2CT}) at the electrode/electrolyte interface. R_S is the series resistance of the device, which includes contributions from the FTO glass current collector. *CPE1* and *CPE2* are the constant phase element and Z_W is the finite Warburg impedance element [33].

Table 3. EIS parameters of DSSCs fabricated with co-sensitized photoanodes.

Co-sensitized TiO_2 photoanode	R_S (Ω)	R_{1CT} (Ω)	R_{2CT} (Ω)	Z_W (Ω)
NP/NP	30.2	58.6	62.1	16.2
NP/NF/NP	18.2	24.5	60	52.9

Impedance parameters of the DSSCs estimated from the above equivalent circuit are listed in the table 3. DSSCs fabricated with triple layered structure shows a lower series resistance (R_S) and a lower charge transfer resistance R_{2CT} compared to the corresponding values obtained for the DSSCs with NP/NP photoanode. Therefore, the rate of electron transfer at the photoanode/electrolyte interface is higher in the DSSCs with triple layer photoanode leading to a higher photocurrent density. Moreover, low value of the charge transfer resistance at the electrolyte/Pt counter electrode interface (R_{1CT}) and the high value of Z_W of the DSSC with NP/NF/NP structure indicate that the oxidation and reduction reaction might be faster in the device than the

DSSC with NP/NP photoanode, as observed by Kim *et al* [34]. Therefore, EIS data are in correlation with the increase in the efficiency due to the enhancement in both J_{SC} and V_{OC} of the DSSC with NP/NF/NP photoanode.

4. Conclusion

In this study we have fabricated and tested DSSCs with triple layered TiO_2 NP/NF/NP composite photoanode sensitized with EY synthetic dye and revealed that the overall efficiency of the device can be improved dramatically by the in-cooperation of a TiO_2 NF layer in triple layer photoanode structures. The overall efficiency of DSSC has been enhanced approximately by 98%. This dramatic enhancement in the overall efficiency could be due to the remarkable enhancement in the light harvesting by absorption due to internal scattering of the photoanode with NF layer, as confirmed by the remarkable increment in the photocurrent density. The overall interfacial resistance of the DSSC has also been reduced by introducing this NF layer to the conventional photoanode structure as confirmed by the EIS measurements.

References

[1] Hagfeldt A, Boschloo G, Sun L, Kloo L and Pettersson H 2010 *Chem. Rev.* **110** 6595
[2] Liu Z H, Su X J, Hou G L, Bi S, Xiao Z and Jia H P 2012 *J. Power Sources* **218** 280
[3] Zhu K, Kopidakis N, Neale N R, De-Lagemaat J V and Frank A J 2006 *J. Phys. Chem. B* **110** 25174
[4] Roy P, Albu A P and Schmuki P 2010 *Electrochem. Commun.* **12** 949
[5] Huang Q, Zhou G, Fang L, Hu L and Wang Z S 2011 *Energy Environ. Sci.* **4** 2145
[6] Peter L M 2011 *J. Phys. Chem. Lett.* **2** 1861
[7] Deepak T G, Anjusree G S, Thomas S, Arun T A and Nair S V 2014 *RSC Adv.* **4** 17615
[8] Qiu Y C, Chen W and Yang S H 2010 *Angew. Chem. Int. Ed.* **49** 3675
[9] Yang L, Lin Y, Jia J G, Xiao X R, Li X P and Zhou X W 2008 *J. Power Sources* **182** 370
[10] Ito S, Murakami T N, Comte P, Liska P, Grätzel C, Nazeeruddin M K *et al* 2008 *Thin Solid Films* **516** 4613
[11] Miao Q Q, Wu L Q, Cui J N, Huang M D and Ma T 2011 *Adv. Mater.* **23** 2764
[12] Son M K, Seo H, Kim S K, Hong N Y, Kim B M, Park S *et al* 2012 *Int. J. Photoenergy* **2012** 480929
[13] Liu Z H, Su X J, Hou G L L, Bi S, Xiao Z and Jia H P 2012 *J. Power Sources* **218** 280
[14] Li W, Yang J, Jiang Q, Luo Y, Hou Y, Zhou S *et al* 2015 *J. Power Sources* **284** 428
[15] Yang L and Leung W W 2011 *Adv. Mater.* **23** 4559
[16] Mohammadpour F and Moradi M 2015 *Mater. Sci. Semicond. Process.* **39** 255
[17] Swathy K S, Abraham P A, Panicker N R, Pramanik N C and Jacob K S 2016 *Procedia Technol.* **24** 767
[18] Dissanayake M A K L, Divarathna H K D W M N, Dissanayake C B, Senadeera G K R, Ekanayake P M P C and Thotawattage C A 2016 *J. Photochem. Photobiol. A: Chem.* **322** 110
[19] Dissanayake M A K L, Jaseetharan T, Senadeera G K R and Thotawatthage C A 2018 *Electrochim. Acta* **269** 172
[20] Dissanayake M A K L, Sarangika H N M, Senadeera G K R, Divarathna H K D W M N R and Ekanayake E M P C 2017 *J. Appl. Electrochem.* **47** 239
[21] Kumar A S, Balaji D, Kumar J R and Babu S M 2009 *Appl. Sci.* **1** 186
[22] Guo M, Diao P, Ren Y-J, Meng F, Tian H and Cai S M 2005 *Sol. Energy Mater. Sol. Cells* **88** 23
[23] Chen Y, Zeng Z, Li C, Wang W, Wang X and Zhang B 2005 *New J. Chem.* **29** 773
[24] Chang H, Kao M-J, Chen T L, Chen C H, Cho K C and Lai X R 2013 *Int. J. Photoenergy* **1** 159502
[25] Kumar K K A and Senthilselvan S J 2019 *Mater. Sci. Semicond. Process.* **96** 104
[26] Rangel D, Gallegos J C, Vargas S, García F and Rodríguez R 2019 *Results Phys.* **12** 2026
[27] Sundrarajan M, Bama K, Bhavani M, Jegatheeswaran S, Ambika S, Sangili A *et al* 2017 *J. Photochem. Photobiol. B: Biol.* **171** 117
[28] Chen J, Song J L, Sun X W, Deng W Q, Jiang C Y, Lei W *et al* 2009 *Appl. Phys. Lett.* **94** 153115
[29] Shen Q, Kobayashi J, Diguna L J and Toyoda T 2008 *J. Appl. Phys.* **103** 084304
[30] Lee Y L, Huang B M and Chien H T 2008 *Chem. Mater.* **20** 6903
[31] Zaban A, Greenshtein M and Bisquert J 2003 *J. ChemPhysChem* **4** 859
[32] Hod I, González-Pedro V, Tachan Z, Fabregat-Santiago F, Mora-Sero I, Bisquert J *et al* 2011 *J. Phys. Chem. Lett.* **2** 3032
[33] Wang Q, Moser J E and Gratzel M 2005 *J. Phys. Chem. B* **109** 14945
[34] Kim H J, Kim D J, Rao S S, Savariraj A D, Kyoung S K, Son M K *et al* 2014 *Electrochim. Acta* **127** 427